FULL PAPER

Ruthenium Nanoparticles Supported onto Carbon Microfibers for Hydrogen Evolution Electrocatalysis

Jordi Creus[a,b,c], Laura Mallón[a,b,c], Nuria Romero[a], Roger Bofill[a], Alicia Moya[d], Jose L. G. Fierro[e], Rubén Mas-Ballesté*[d,f], Xavier Sala[a], Karine Philippot*[b,c], Jordi García-Antón*[a]

Abstract: Four different cathodes for the hydrogen evolution reaction (HER) have been developed by the decoration of commercial carbon microfibers with Ru nanoparticles (Ru NPs). Two types of carbon fibers have been used: pristine, as-received, carbon fibers (pCF) and carbon fibers modified by an oxidative treatment that led to the functionalization of their surface with carboxylic groups (fCF). The decoration of these CFs with Ru NPs has been performed by two different methodologies based on the organometallic approach: direct synthesis of Ru NPs on top of the CFs (*in-situ* Ru NPs) or impregnation of the CFs with a colloidal solution of preformed Ru NPs stabilized with 4-phenylpyridine (RuPP NPs; *ex-situ* Ru NPs). The electrocatalytic performance of these four cathodes (*ex-situ* RuPP@pCF and RuPP@fCF; *in-situ* Ru@pCF and Ru@fCF) for the HER has been studied in acidic conditions. The results obtained showed that both the nature of the NPs and of the carbon fibers play a key role on the stability and activity of the hybrid electrodes.

Introduction

During the last decades, the world energy demand has exponentially increased, [1] meaning that there is a huge requirement of energy sources to fulfil this necessity. Additionally, the abusive use of fossil fuels, which are actually running out, has been damaging the atmosphere and ozone layer, leading to environmental and health issues.[2] Thus, an alternative to carbon-based fuels needs to be found, which must be clean and renewable. Hydrogen has been thoroughly studied as an energy vector due to its interesting properties as energy carrier[3] and the cleanness of its consumption. Although nowadays the main production process is the steam reforming from natural gas, water splitting (WS) has proved to be a promising renewable method for the formation of H_2 through the Hydrogen Evolution Reaction (HER) and the redox counterpart Oxygen Evolution Reaction (OER).[4]

The evolution of H_2 from water through the reduction of protons is achieved mainly with Pt-based catalysts, which are considered the state-of-the-art catalysts for this reaction. This relies in the fact that the Pt-H bond is strong enough to be stable but still weak enough to be easily broken and facilitate H_2 formation. [5] The scarcity and high cost of Pt, as well as its low stability in alkaline media,[5b] encourages the scientific community to investigate other metals. [6] In acidic media, first-row transition metals show low stability, presumably due to acid corrosion, and their overpotentials under basic conditions are far to be competitive with those of Pt. [7] In contrast, Ru seems an ideal candidate because i) the Ru-H bond energy is slightly weaker than the Pt-H one, what has no significant influence on the overpotentials in comparison to Pt-based catalysts, and ii) it presents high stability both at acidic and basic pH.[5] Additionally, its price is only 1/4th of that of Pt, thus increasing the HER cost-efficiency of Ru-based species.

The use of NPs as (electro)catalysts for the HER has been gathering more and more attention in the last years. This interest arises from the particular properties of NPs that combine features from both homogeneous and heterogeneous systems. This includes a higher stability compared to molecular complexes and intrinsically high surface/volume ratio. [8] In contrast, electron transfer in NP-based electrocatalysts is typically not as good as it can be with molecular complexes, being that solved with the immobilization onto solid supports and electrodes, as e.g. highly-conductive carbon-based materials,[9] silica,[10] oxides,[11] or even directly onto glassy carbon (GC) electrodes.[12]

NPs size, shape, structure and homogeneity are crucial characteristics affecting the performance of nanosized catalytic systems. A good control on the surface environment and NPs structure is required in the methodology used for the synthesis to correlate the physical/chemical properties of the system and the catalytic output, and hence for the future rational design of new active and stable nanometric materials. In this sense, and as a result of the method used for their synthesis and stabilization, we have recently reported two different nanomaterials displaying interesting activities in the electrocatalytic HER.[13,14] This method, the so-called organometallic approach, permits to have very small NPs of controlled dimension and narrow size-distribution, applying mild synthetic reaction conditions and avoiding the use of salts, thus controlling their surface environment and their catalytic properties.[15] This favours the study and understanding of the NPs catalytic performance and its relationship with their surface properties.

[a]   Departament de Química, Universitat Autònoma de Barcelona, Cerdanyola del Vallès, 08193 Barcelona, Spain.
        Email: jordi.garciaanton@uab.es
[b]   LCC (Laboratoire de Chimie de Coordination), 205 Route de Narbonne, BP44099, 31077 Toulouse Cedex 4, France.
        Email: karine.philippot@lcc-toulouse.fr
[c]   Université de Toulouse III, UPS, INPT, 31077 Toulouse Cedex 4, France.
[d]   Department of Inorganic Chemistry (module 07), Facultad de Ciencias, Universidad Autónoma de Madrid, Madrid, Spain
   Email: ruben.mas@uam.es
[e]   Instituto de Catálisis y Petroleoquímica, CSIC, Madrid, Spain
[f]   Institute for Advanced Research in Chemical Sciences (IAdChem), Universidad Autónoma de Madrid, Madrid, Spain

        Supporting information for this article is given via a link at the end of the document.

FULL PAPER

In a recent report,[16] we studied carbon microfibers (CFs) obtained from the pyrolysis of polyacrylonitrile (PAN).[17] They present a graphene-like structure including pyridyl moieties that can be easily oxidized to generate carboxylic acid groups in a limited extent. Such oxidative functionalization affords differentiated surface properties, *i. e.* nicotinic fragments as catalytic centres for the HER, but with maintained bulk electric conductivity. The use of CFs (pristine or oxidized) as supports for Ru NPs allows the fabrication of stable and high surface area functionalized electrodes. In this work, carbon microfibers are used as supports of Ru-based NPs prepared either *in-situ* onto the CFs surface or *ex-situ*. The resulting hybrid materials are investigated in this work as cathodes in the HER. The obtained results demonstrate that the nature of the support (oxidized compared to bare CFs) as well as the pre-stabilization of the NPs (*in-situ* compared to *ex-situ* synthesized NPs) play a key role in the observed HER electroactivity, and more importantly, in the stability of the hybrid electrode materials synthesized.
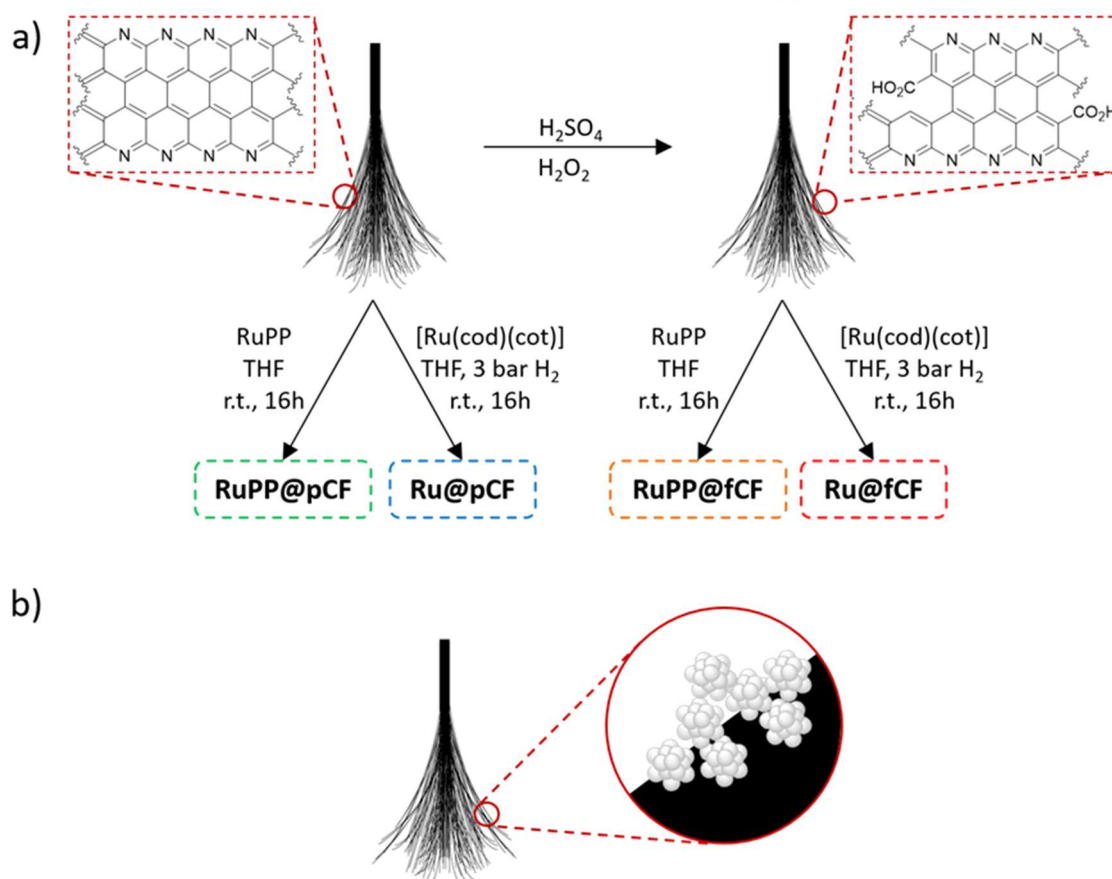
Scheme 1. a) Schematic representation of the surface chemical composition of pristine carbon fibers (pCF; top left) and functionalized carbon fibers (fCF; top-right) and experimental procedure for the deposition / synthesis of Ru NPs onto the surface of the carbon fibers. b) Schematic representation of the surface of the carbon fibers once the Ru NPs have been deposited / synthesized.

Results and Discussion

### Synthesis and characterization.
Four hybrid materials have been prepared for the study of their catalytic performance in the HER (Scheme 1). First, two different supports were used: pristine CFs (pCF) and functionalized CFs (fCF). Pristine CFs present a clean surface, as described previously;[16] in contrast, fCF present carboxylic acid groups at their surface as a result of the modification treatment of pCFs by oxidation in a 1:1 mixture of H_2SO_4/H_2O_2. During this oxidation process, the graphitic regions of the carbon fibers were not massively altered and, therefore, electric conductivity was

preserved. These modified microfibers have been shown to be electroactive catalysts towards the HER[16] thanks to the new carboxylic acid moieties present (see Figures S1-S3 in the SI for TEM images of pCF and fCF, and their LSV curves before and after bulk electrolysis at η = 250 mV in a 1 M H_2SO_4 solution).

As shown in Scheme 1(a), pCF and fCF were decorated with Ru nanoparticles (Ru NPs) following two different methodologies, both based on the organometallic approach for the synthesis of NPs.[15] Thus, a certain amount of NPs can be loaded onto the fibers surface, which can have different surface environments depending on the synthetic method used. The 1st methodology is an *in-situ* synthesis. in which Ru NPs have been prepared by decomposing under hydrogen 10 mg of [Ru(cod)(cot)] (cod: 1,5-cyclooctadiene; cot: 1,3,5-cyclooctatriene) in the presence of the

CFs (90 mg; THF, r.t., 3 bar H_2). Both (pCF and fCF) were placed at the same time in the reaction vessel to ensure the same reaction conditions, resulting in a final Ru/CF ratio of ≈ 0.6 wt.% for each case. By this way, naked metal atoms released from the decomposition of the Ru precursor nucleated directly onto the electrode surface (Scheme 1(b)). The NPs obtained under these conditions can only be stabilized by the different possible NP-CF(surface) interactions and with solvent molecules (THF). The 2nd methodology is an *ex-situ* approach. In this case, the Ru particles (RuPP NPs) were pre-synthesized by decomposing [Ru(cod)(cot)] at r.t., under H_2, in THF and in the presence of 0.2 eq. of 4-phenylpyridine (PP) as stabilizer, as recently reported.[14] The overnight soaking of xCF (x = p, f) into the crude colloidal RuPP NPS dispersion led to the attachment of the NPs onto the CFs surface. The main difference with the 1st method is the presence of 4-phenylpyridine at the surface of the Ru NPs when deposited onto the CF supports. As previously published,[14] the RuPP NPs supported onto a glassy carbon disk electrode have shown large current intensities at low overpotentials for the electrocatalytic HER, with excellent stability after 12-h of continuous catalysis both under strong acidic and basic conditions (1 M H_2SO_4 and 1 M NaOH, respectively).
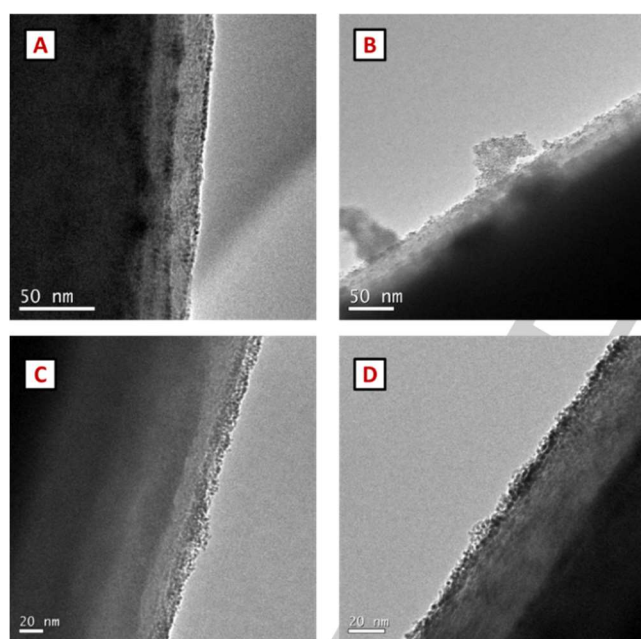
Figure 1. Representative TEM images of the hybrid materials a) **Ru@pCF**, b) **Ru@fCF**, c) **RuPP@pCF** and d) **RuPP@fCF**.

The combination of the two different supports and two synthetic methodologies allowed obtaining four different hybrid materials, **Ru@pCF**, **Ru@fCF**, **RuPP@pCF** and **RuPP@fCF**, which have been characterized by TEM, XPS and ICP. The TEM analysis of these systems (Figure 1 and Figures S4-S7) confirmed in all cases the presence of very small particles onto the surface of the CFs. Even if some agglomerates constituted of very small NPs can be observed in a few zones of the microfibers, the Ru NPs mostly form a homogeneous layer at their surface, except for the

Ru@fCF system, for which NPs agglomeration has been repeatedly observed. This parameter could be significant when testing the electrocatalytic performance of this particular system. Given the difficulty to take images of NPs of less than 2 nm on top of CFs of ≈8 μm of diameter, the mean size of the Ru NPs was difficult to measure and was estimated to be comprised within the 1.0-1.8 nm range for the four cases (see Table 1). XPS analyses (Figure 2) show that the Ru NPs contain two phases, metallic Ru and RuO_2, due to a partial oxidation of the surface of the NPs when exposed to air, with Ru $3d_{5/2}$ peaks centred at 279.8 eV (metallic Ru) and 280.8 eV (RuO_2).[18] ICP data of the whole material slightly varies from one sample to another, being the Ru content lower than 2% in all cases, as expected if we take into account the relative thickness of the fibers compared to those of the NPs, thus implying a high C content (Table 1).

Table 1. Mean size and electrochemical HER performance of Ru@pCF, Ru@fCF, RuPP@pCF and RuPP@fCF in 1 M H_2SO_4 aqueous solution. Ø = mean size of the Ru NPs; η_0 = onset overpotential; η_{10} = overpotential at $|i_{cat}|$ = 10 mA·mg^{-1}; Ru wt. % = weight percentage of Ru in the sample, η_1 = overpotential at $|i_{Ru}|$ = 1 A·mg^{-1}, % i_{cat} = percentage of current intensity at η = 200 mV after a 2 h electrolysis.

System	Ø (nm)	η_0 (mV)	η_{10} (mV)	Ru wt.%	η_1 (mV)	% i_{cat}[a]
pCF	-	220	-	-	-	-
fCF	-	180	-	-	-	-
RuPP	1.5 ± 0.3	0	20[b]	85	90	99[b]
Ru@pCF	1.4 ± 0.4	70	265	0.57	240	34
Ru@fCF	1.0 ± 0.2	30	235	0.65	210	16
RuPP@pCF	1.8 ± 0.3	5	225	0.47	150	95
RuPP@fCF	1.5 ± 0.7	0	180	1.10	190	40

[a] %i_{cat} calculated by dividing i_{cat} (η = 200 mV) at t = 2 h by the value at t = 0 as short-term stability data. [b] Data for RuPP is taken from reference 14 for $|j|$ = 10 mA·cm^{-2} instead of $|i_{cat}|$= 10 mA·mg^{-1}.

Electrocatalytic HER performance.
For the electrocatalysis experiments, the electrodes were built with 1 mg of each hybrid material to avoid reproducibility issues because of the aggregation of the microfibers when used in higher amounts, as well as to minimize the effect of accumulation of H_2 bubbles, since the gas is produced as big bubbles that block the electrode surface and diminish its electrochemical response. For further details on the electrode preparation, see the Experimental Section. The electrodes were tested under reductive potentials in a two-compartment cell containing 1 M H_2SO_4. First, a change on the current intensity has been observed at potentials below 0 V vs. RHE, which is the thermodynamic potential for the HER (E_{therm}). The current intensity, which is referenced per mg of material as i_{cat} = [mA·mg$_{cat}$$^{-1}$], has been also normalized by the Ru wt.% in each case in order to be able to compare the catalytic activity between samples with different Ru loadings, and the new values were labelled as i_{Ru} = [A·mg$_{Ru}$$^{-1}$]. Table 1 summarizes the electrochemical performance of the four different systems displayed in Figure 3.
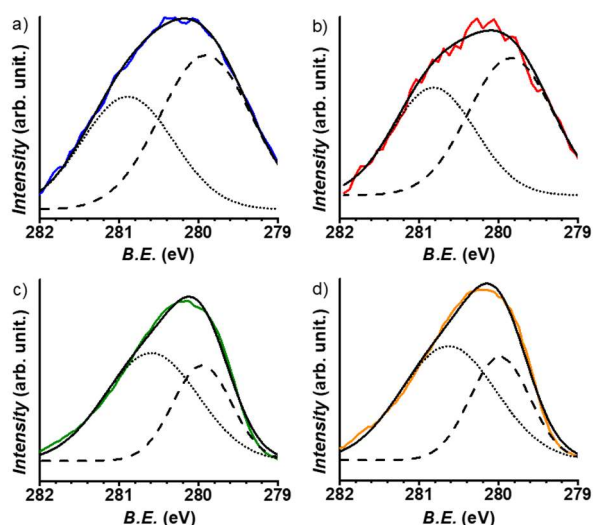
Figure 2. XPS analysis of a) **Ru@pCF** (blue, top-left), b) **Ru@fCF** (red, top-right), c) **RuPP@pCF** (green, bottom-left) and d) **RuPP@fCF** (orange, bottom-right). Metallic-Ru component (Ru $3d_{5/2}$-279.8 eV, dashed black), RuO$_2$-component (Ru $3d_{5/2}$-280.8 eV, dotted-black), envelope (bold).

First of all, the onset overpotential, η_0, is close to 0 mV for **RuPP@pCF** and **RuPP@fCF**, confirming a similar behaviour to that observed for RuPP NPs onto glassy carbon, as previously described (see RuPP-GC material in ref 14). This value is considerably lower than that observed for the CFs (catalytically inactive) and for the oxidized CFs (catalytically active). Thus, considering that similar values of η_0 are observed using both materials, we can conclude that, for RuPP@xCF electrodes, there is no influence of the carbon support in the catalytic activity of the generated hybrid materials, where the RuPP NPs work as catalytic centres independently of the support. In contrast, **Ru@pCF** and **Ru@fCF** show higher η_0 (70 and 30 mV, respectively) than RuPP@xCF, and comparable to the η_0 values reported in the literature for C-supported Ru NPs.[9] From these values, two main conclusions can be deduced. First, the presence of the 4-phenylpyridine ligand as stabilizer has a positive impact on the catalytic activity. Second, it seems that somehow there is a synergistic effect arising from the coexistence of Ru catalytic NPs and active organic fragments in **Ru@fCF** in comparison with **Ru@pCF**.

Stability studies were carried out through long term bulk electrolysis experiments with maintained $|i_{cat}| \approx 10$ mA·mg$_{cat}^{-1}$ in all cases. In the last column of Table 1, % i_{cat} (t = 2 h) values, defined as the remaining current percentage measured by LSV at a specific overpotential (η = 200 mV) after 2 h of catalytic turnover, allow a comparison of the stability of the four systems (graphical data can be found in Figure 4). While **Ru@fCF** shows a decrease of its i_{cat} down to 16% in 2 h (i_{cat} = -5.0 mA·mg^{-1} (t=0) vs. -0.8 mA·mg^{-1} (t=2 h), **Ru@pCF** still keeps 34% of i_{cat} after the same time (i_{cat} = -1.8 mA (t=0) vs. -0.6 mA (t=2 h)) and requires 5 h to

lose the same percentage of activity. Likewise, **RuPP@fCF** requires 2 h to lose 60% of the i_{cat} (i_{cat} = -14.5 mA·mg^{-1} (t=0) vs. -5.7 mA·mg^{-1} (t=2 h)). Remarkably, **RuPP@pCF** is stable under catalytic conditions, nearly maintaining its initial activity after 2h (i_{cat} = -8.6 mA·mg^{-1} (t=0) vs. -7.8 mA·mg^{-1} (t=2h)).
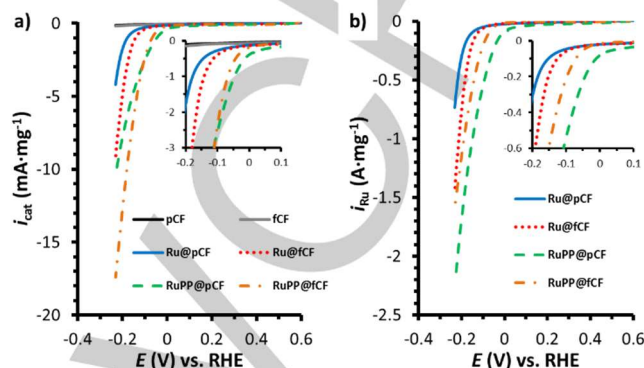
Figure 3. Polarization curves of **Ru@pCF** (blue solid line), **Ru@fCF** (dotted red line), **RuPP@pCF** (dashed green line), **RuPP@fCF** (dash-dotted orange line), pCF (black solid line) and fCF (grey solid line) in 1M H$_2$SO$_4$ normalized by mg of material (left) and by mg of Ru (right).

To unravel the causes influencing the stability of the four systems, TEM analyses of the electrode materials after the 2h bulk electrolysis experiments were performed. Comparing TEM images (Figures S8-S11), there is visual evidence that the *in-situ* prepared Ru@xCFs systems suffer significant leaching during the catalytic process, leaving cleaner surfaces of the CFs for both **Ru@pCF** and **Ru@fCF** (Figures S8 and S9, respectively), but that nevertheless also contain some agglomerates, which have been formed during the catalytic reaction. This trend is confirmed by the EDX analysis of the surface of **Ru@pCF** and **Ru@fCF** (Figures S8 and S9, respectively), showing almost no presence of Ru, in agreement with the electrocatalytic results. In contrast, the two RuPP-based systems (**RuPP@pCF** and **RuPP@fCF**) present higher loadings of Ru NPs on the surface of the fibers after catalysis (Figures S10 and S11, respectively) than the Ru@xCF systems, with very small NPs along the CFs surface and almost no agglomeration observed. EDX analyses (Figures S10 and S11, respectively) confirm, in this case, the presence of Ru throughout the surface. In our previous publication,[14] RuPP NPs deposited onto a GC electrode with no gluing agent added were held at a constant current density of j = −10 mA·cm^{-2} in a 12 h current-controlled experiment in the same acidic conditions as in the present work (1 M H$_2$SO$_4$). Moreover, RuPP NPs presented no deactivation signs, and displayed identical LSV polarization curves before and after the catalytic turnover. Considering these previous results, it is clear that RuPP NPs are stable under the applied catalytic conditions. Consequently, the deactivation observed for **RuPP@fCF** can be attributed to a mechanical instability of the NPs. Thus, there may occur a continuous loss of NPs from the surface of the CFs, which may settle down at the bottom of the reaction vessel as detached NPs.

FULL PAPER

The Faradaic efficiency (FE, %) of the hybrid materials has been evaluated by performing 10-min bulk electrolysis experiments with an H_2-Clark sensor which allows the *in-situ* detection of the generated H_2. The charge passed through the system was transformed first to moles of electrons by the Faradaic constant, and then to theoretical H_2 moles by taking into account that the formation of hydrogen gas requires two electrons per molecule. The experimental data for H_2 generation were extracted from the Clark sensor calibrating the electrochemical signal (mV) with different amounts of 99% pure H_2 and extrapolating the obtained data. The FE was estimated by dividing the value detected by the H_2-Clark sensor by the charge value at the end of the experiment, confirming that almost quantitative number of electrons were specifically devoted to the reduction of protons and not to other side processes (see Figure S12).
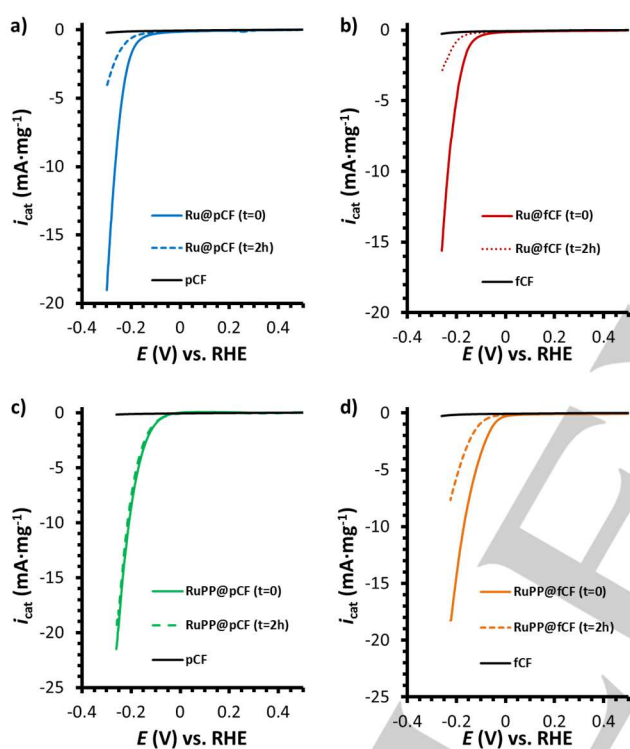
Figure 4. LSV curves for a) **Ru@pCF**, b) **Ru@fCF**, c) **RuPP@pCF** and d) **RuPP@fCF** recorded along a bulk electrolysis experiment in 1 M H_2SO_4 to study the stability of the different systems. An E_{app}= -250 mV was used for the Ru@xCF systems to reach $i_{cat} \approx$ 10 mA·mg^{-1} during the electrolysis, while an E_{app}= -150 mV was used for the RuPP-based systems.

Altogether, the electrocatalytic results evidence that both the nature of the carbonaceous fibers and the surface environment of the NPs play a key role on the activity and stability of the hybrid materials used as cathodes in the HER. Considering the activity of the hybrid materials, *ex-situ* RuPP-systems (**RuPP@pCF** and **RuPP@fCF**) reach higher intensities at low overpotentials than the *in-situ* Ru-based ones (**Ru@pCF** and **Ru@fCF**). This behaviour confirms the positive effect of the interaction of the 4-phenylpyridine ligand with the NPs regarding their catalytic

performance, as previously stated.[14] If we take into account the relative stabilities observed in the bulk electrolysis experiments, the *ex-situ* RuPP-systems (**RuPP@pCF** and **RuPP@fCF**) are more stable (95% and 40% activity maintained after 2-h, respectively) than the Ru-based ones (**Ru@pCF** and **Ru@fCF**; 34% and 16% activity maintained after 2-h, respectively). We propose that the improved stability of the RuPP-based hybrid materials derives from the properties of the 4-phenylpyridine ligand at the Ru NPs surface which, besides assuring the stabilization of the NPs, can also favour their anchoring at the surface of the support, probably through π-stacking interactions with the surface of the CFs. If we only compare the RuPP-systems, the carboxylate groups in the **RuPP@fCF** electrode might hamper these π-stacking interactions, thus being detrimental for the mechanical stability of the Ru NPs at the surface of this particular C-based electrode.

Conclusions

Four different heterogeneous hybrid cathodes based on the decoration of CFs with Ru NPs have been designed and tested for the electrocatalytic HER. On the one hand, two types of CFs have been used: pristine (**pCF**) or functionalised (after an oxidative treatment that affords surface carboxylic groups; **fCF**) fibers. On the other hand, two types of Ru NPs prepared through the organometallic synthesis method have been loaded onto the surface of the CFs: Ru NPs prepared *in-situ* on top of the CFs or Ru NPs synthesized *ex-situ* with 4-phenylpyridine (PP)[14] and subsequently deposited onto the surface of the CFs by an impregnation method. By this way, we had in hands two *ex-situ* (**RuPP@pCF** and **RuPP@fCF**) and two *in-situ* (**Ru@pCF** and **Ru@fCF**) cathodes for the electrocatalytic studies (Scheme 1).
The electrochemical studies clearly indicate that the nature of the carbon fibers (pristine or carboxylic acid-functionalized) and the nature of the Ru NPs (*in-situ* or *ex-situ*) are decisive on the activity and stability of each of the four cathodes for the HER.
More specifically, both RuPP@xCF electrodes present η_0 overpotentials close to 0 mV, similar to those obtained for RuPP NPs deposited onto a glassy carbon electrode. In this case, thanks to the outstanding electrocatalytic properties of the RuPP NPs, the nature of the carbon fibers is not decisive in the final output. On the other hand, the nature of the carbon fibers is indeed significant for the activity of Ru@xCF hybrid systems: **Ru@fCF** present a much lower η_0 overpotential (30 mV) than **Ru@pCF** (70 mV). This is in agreement with the results previously obtained with pristine or functionalized CFs not decorated with Ru NPs. This observation suggests that for **Ru@fCF** some degree of cooperation exists between the Ru NPs and the nicotinic moieties, which have been recently suggested as catalytic centres in non-decorated fCFs.[16]
Additionally, pCFs improve the stability of the cathodes, suggesting that the carboxylic groups onto the surface of the fCFs prevent the stabilization of the Ru NPs by the pyridyl-based structure of the CFs. If we consider the nature of the Ru NPs, RuPP-based cathodes (RuPP@xCF; x = p or f) present much higher stabilities and activities than those obtained with Ru NPs

synthesized *in-situ* (Ru@xCF; x = p or f). These results confirm the positive effect of the 4-phenylpyridine capping ligand, not only acting as a stabilizing agent for the Ru NPs but also as a gluing agent of the nanocatalysts onto the C-based support, conferring mechanical stability to the hybrid cathode.

Overall, the results reported herein demonstrate the viability of hybrid materials composed by CFs and Ru NPs as remarkable electrocatalysts for the HER. The best compromise between activity and stability is achieved by using pristine CFs and Ru NPs stabilized by the surface coordination of 4-phenylpyridine. This is probably indicative of a better π-π interaction between the aromatic 4-phenylpyridine ligand and the graphitic region of the carbon fibers, which, in turn, can be hindered by the oxidative derivatization of the carbon material.

In conclusion, we designed electrodes with high surface area from a material with a low metal content (0.5% wt) on a macroscopic cheap substrate, allowing thus a step further towards the massive and economic production of hydrogen under benign conditions.

Experimental Section

Materials and reagents. All operations for the synthesis of the CF-supported Ru NPs were carried out using standard Schlenk tubes, Fisher–Porter bottle techniques or in a glove-box (MBraun) under argon atmosphere. Solvents (THF and pentane) were purified before use by filtration on adequate columns in a purification apparatus (MBraun) and handled under argon atmosphere. Solvents were degassed before use according to a freeze–pump–thaw process. The ruthenium precursor, [Ru(cod)(cot)], was purchased from Nanomeps-Toulouse. Hydrogen gas (Alphagaz) was purchased from Air Liquide. 4-Phenylpyridine used as stabilizer was purchased from Sigma-Aldrich and used as received. High purity deionized water was obtained by passing distilled water through a nanopore Milli-Q water purification system. Pristine carbon fibers were purchased from ClipCarbono[19].

CF electrode preparation. Carbon fibers were washed by sonication for 10–15 min in isopropanol and dried with a heat gun. The **fCF** material was prepared by exposing the **pCF** ready-made electrodes to commercial sulfuric acid (98 %) at r.t. during 30 min under stirring. Then, the material was placed into a H_2SO_4/H_2O_2 1:1 mixture. The H_2O_2 was fresh and the mixture with H_2SO_4 was prepared a few minutes before use. The electrodes were washed and sonicated in distilled water to remove all acid traces among fibers; this required several washing cycles. When the pH of the water was constant, the electrodes were sonicated for 10–15 min in isopropanol and dried with a heat gun. The carbon fiber electrodes were hand-made prepared using a short copper wire, ≈50 cm long carbon fibers and some Teflon tape to tight everything together. The CFs electrodes contain 7 bundles of 3000 filaments (21000 filaments) of ≈8 μm diameter and 6 cm length each. The fibers were bended so each electrode contained the double of the filaments (42000). Only 2 cm were exposed for the synthesis of the NPs and electrode usage. These electrodes weighted approximately 90 mg. After deposition of the NPs but before electrochemical evaluation, these electrodes were cut in 3-cm-long filaments (half fiber), and 1-mg-samples were attached to a Cu tape together with a Cu-wire, still ensuring 2 cm were left for catalysis evaluation.

Ru@xCF, x = pristine (p) or functionalized (f). 2 cm of xCFs were soaked in a 10 mL THF solution containing [Ru(cod)(cot)] (10 mg, 0.026 mmol) inside a Fisher-Porter bottle. 3 bar of H_2 were introduced and the reaction mixture was stirred at r.t. overnight. After depressurization, the

hydrogen was evacuated under vacuum and the solvent removed through a cannula. The resulting CF materials were rinsed with pentane and dried under vacuum. **Ru@pCF.** TEM: Ø = 1.4 ± 0.4 nm. ICP(Ru%) = 0.57%. **Ru@fCF.** TEM: Ø = 1.0 ± 0.2 nm. ICP(Ru%) = 0.65%.

RuPP@xCF, x = pristine (p) or functionalized (f). 2 cm of xCFs electrodes were soaked overnight in a THF (10 mL) crude dispersion of **RuPP** NPs[14] inside a Fisher-Porter bottle. Then, the supernatant was removed through cannula and the resulting CF materials were rinsed with pentane (3x10 mL) and dried under vacuum. **RuPP@pCF.** TEM: Ø = 1.8 ± 0.3 nm. ICP(Ru%): 0.47%. **RuPP@fCF.** TEM: Ø = 1.5 ± 0.7 nm. ICP (Ru%): Ru@fCF: 1.10%.

Characterization

Transmission Electron Microscopy (TEM) and High-Resolution Electron Microscopy (HREM). TEM and HREM observations were performed at the "Centre de Microcaractérisation Raymond Castaing" in Toulouse (UMS-CNRS 3623) and at the "Servei de Microscòpia Electrònica" of the UAB. Samples for TEM and HREM analyses were prepared by deposition of several CFs onto a holey carbon-covered copper grid. TEM and HREM analyses were performed on a MET JEOL JEM 1011 microscope operating at 100 kV with a resolution point of 0.45 nm and a JEOL JEM-ARM 200F microscope working at 200 kV with a resolution point lower of 0.19 nm, respectively. TEM allowed to evaluate the particle size, size distribution and morphology. Enlarged micrographs were used for treatment with ImageJ software to obtain a statistical size distribution and the NP mean diameter. The analyses were done by assuming that the NPs were spherical. NP sizes are quoted as the mean diameter ± the standard deviation.

Inductive-Coupled Plasma (ICP-OES). ICP-OES measurements were performed at the "Servei d'Anàlisis Químic" (SAQ) in the UAB, on an Optima 4300DV Perkin-Elmer system. Solid samples were prepared by digesting 1 mg of the hybrid CFs with *aqua regia* under microwave conditions followed by a dilution of the mixture with HCl 1% (v/v). Liquid samples were directly diluted with HCl 1% (v/v).

X-Ray Photoelectron Spectroscopy (XPS). Measurements were performed at the Catalan Institute of Nanoscience and Nanotechnology (ICN2) in Barcelona with a Phoibos 150 analyzer (SPECS GmbH, Berlin, Germany) in ultra-high vacuum conditions (base pressure $5 \cdot 10^{-10}$ mbar) with a monochromatic aluminium Kalpha x-ray source (1486.74 eV). The energy resolution was measured by the FWHM of the Ag $3d^{5/2}$ peak which for a sputtered silver foil was 0.62 eV.

Electrochemical measurements. All the electrochemical experiments were performed using a BioLogic SP-150 potentiostat. Solutions were degassed before the electrochemical analysis with a N_2 flow. IR drop was automatically corrected at 85 % using the Biologic EC-Lab software for cyclic voltammetry and chronoamperometry. 1 M H_2SO_4 solution was prepared by mixing 56.1 mL of 95-97 % H_2SO_4 in 1 L of Mili-Q water. A Pt grid was used as a counter electrode (CE) and an Ag/AgCl (KCl sat.) electrode was used as a reference electrode (RE). All data were transformed to RHE by adding +0.20 V. A 10 mL two-compartment cell with a separation membrane between the two compartments was used. Both compartments were filled with 8 mL of 1 M H_2SO_4 solution and were equipped with a stirring bar. Prior to each measurement, they were purged with N_2 for 15 min. For H_2-monitored bulk electrolysis an Unisense H2-NP Clark electrode was used to measure hydrogen evolution in the gas phase and to calculate the Faradaic efficiency. The Clark electrode was calibrated by adding different volumes of 99% pure hydrogen at the end of

the experiment. The CE was placed in one compartment and the other was provided with the WE, the RE and the Clark electrode.

Linear Sweep Voltammetry (LSV). The system was scanned from E_i = 0.6 V to E_f = -0.4 V at 10 mV/s scan rate unless otherwise stated.

Chronoamperometry. Controlled potential chronoamperometric experiments were performed at E_{app} = -0.25 V and -0.15 V for Ru- and RuPP-CF based systems, respectively.

Acknowledgments

Keywords: Ruthenium • Nanoparticle • HER • Carbon Fiber • Energy
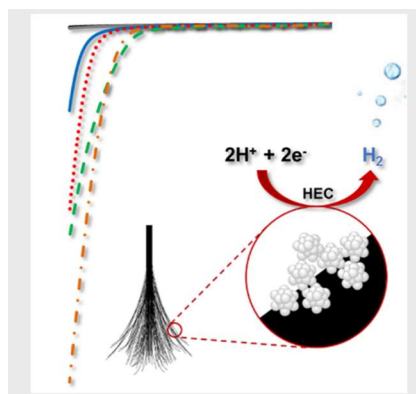
[1] *BP Energy Outlook* **2018**, BP Global.

[2] V. Scott, R. S. Haszeldine, S. F. B. Tett, A. Oschlies, *Nat. Clim. Change* **2015**, *5*, 419-423.

[3] N. S. Lewis, *Nature* **2001**, *414*, 589-590.

[4] S. Berardi, S. Drouet, L. Francàs, C. Gimbert-Suriñach, M. Guttentag, C. Richmond, T. Stoll, A. Llobet, *Chem. Soc. Rev.* **2014**, *43*, 7501-7519.

[5] a) S. Trasatti, *J. Electroanal. Chem.* **1972**, *39*, 163-184; b) C. C. L. McCrory, S. Jung, I. M. Ferrer, S. M. Chatman, J. C. Peters, T. F. Jaramillo, *J. Am. Chem. Soc.* **2015**, *137*, 4347-4357; c) J. K. Norskov, T. Bligaard, A. Logadottir, J. R. Kitchin, J. G. Chen, S. Pandelov, U. Stimming, *J. Electrochem. Soc.* **2005**, *152*, J23-J26.

[6] a) N. Coutard, N. Kaeffer, V. Artero, *Chem. Commun.* **2016**, *52*, 13728-13748; b) A. Eftekhari, *Int. J. Hydrogen Energy* **2017**, *42*, 11053-11077.

[7] a) Y. G. Li, H. L. Wang, L. M. Xie, Y. Y. Liang, G. S. Hong, H. J. Dai, *Am. Chem. Soc.* **2011**, *133*, 7296-7299; b) E. J. Popczun, J. R. McKone, C.G. Read, A. J. Biacchi, A. M. Wiltrout, N. S. Lewis, R. E. Schaak, *J. Am. Chem. Soc.* **2013**, *135*, 9267-9270; c) T. F. Jaramillo, K. P. Jorgensen, J. Bonde, J. H. Nielsen, S. Horch, I. Chorkendorff, *Science* **2007**, *317*, 100−102; d) J. R. McKone, B. F. Sadtler, C. A. Werlang, N. S. Lewis, H. B. Gray, *ACS Catal.* **2013**, *3*, 166-169; e) L. Liao, S. N. Wang, J. J. Xiao, X. J. Bian, Y. H. Zhang, M. D. Scanlon, X. L. Hu, Y. Tang, B. H. Liu, H. H. Girault, *Energy Environ. Sci.* **2014**, *7*, 387-392.

[8] M. Zheng, Y. Li, *J. Mater. Chem.* A **2015**, *3*, 14942-14962.

[9] a) J. Mahmood, F. Li, S. Jung, M. S. Okyay, I. Ahmad, S. Kim, N. Park, H. Y. Jeong, J. Baek, *Nature Nanotech.* **2017**, *12*, 441-446; b) T. Bhowmik, M. K. Kundu, S. Barman, *ACS Appl. Mater. Interfaces* **2016**, *8*, 28678-28688; c) J. Cheng, H. Zhang, H. Ma, H. Zhong, Y. Zou, *Electrchim. Acta* **2010**, *55*, 1855-1861; d) X. Kong, K. Xu, C. Zhang, J. Dai, S. N. Oliaee, L. Li, X. Zeng, C. Wu, Z. Peng, *ACS Catal.* **2016**, *6*, 1487-1492; e) Y. Zheng, Y. Jiao, Y. Zhu, L. H. Li, Y. Han, Y. Chen, M. Jaroniec, S. Qiao, *J. Am. Chem. Soc.* **2016**, *138*, 16174-16181; f) Z. Chen, J. Lu, Y. Ai, Y. Ji, T. Adschiri, L. Wan *ACS Appl. Mater. Interfaces* **2016**, *8*, 35132-35137.

[10] a) Y. Zhang, T. Ren, *Chem. Commun.* **2012**, *48*, 11005-11007; b) N. C. King, C. Dickinson, W. Zhou, D. W. Bruce, *Dalton Trans.* **2005**, *6*, 1027-1032; c) K. P. J. Gustafson, A. Shatskiy, O. Verho, M. D. Kärkäs, B. Schluschass, C. Tai, B. Åkermark, J. Bäckvall, E. V. Johnston, *Catal. Sci. Technol.* **2017**, *7*, 293-299.

[11] a) J. Liu, Y. Zheng, D. Zhu, A. Vasileff, T. Ling, S. Z. Qiao, *Nanoscale* **2017**, *9*, 16616-16621; b) P. Jiang, Y. Yang, R. Shi, G. Xia, J. Chen, J. Su, Q. Chen, *J. Mater. Chem. A* **2017**, *5*, 5475-5485; c) U. Joshi, S. Malkhandi, Y. Ren, T. L. Tan, S. Y. Chiam, B. S. Yeo, *ACS Appl. Mater. Interfaces* **2018**, *10*, 6354-6360; d) L. Zhu, Q. Cai, F. Liao, M. Sheng, B. Wu, M. Shao, *Electrochem. Commun.* **2015**, *52*, 29-33; e) E. Demir, S. Akbayrak, A. M. Önal, S. Özkar, *ACS Appl. Mater. Interfaces* **2018**, *10*, 6299-6308.

[12] a) K. Magdić, K. Kvastek, V. Horvat-Radošević, *Electrochim. Acta* **2015**, *167*, 455-469; b) R. K. Shervedani, A. Amini, *Carbon* **2015**, *93*, 762-773.

[13] S. Drouet, J. Creus, V. Collière, C. Amiens, J. García-Antón, X. Sala, K. Philippot, *Chem. Commun.* **2017**, *53*, 11713-11716.

[14] J. Creus, S. Drouet, S. Suriñach, P. Lecante, V. Colliere, R. Poteau, K. Philippot, J. García-Antón, X. Sala, *ACS Catal.* **2018**, *8*, 11094-11102.

[15] C. Amiens, B. Chaudret, D. Ciuculescu-Pradines, V. Collière, K. Fajerwerg, P. Fau, M. Kahn, A. Maisonnat, K. Soulantica, K. Philippot, *New J. Chem.* **2013**, *37*, 3374-3401.

[16] O. González-del Moral, A. Call, F. Franco, A. Moya, J. A. Nieto-Rodríguez, M. Frías, J. L. G. Fierro, M. Costas, J. Lloret-Fillol, J. Alemán, R. Mas-Ballesté, *Chem. Eur. J.* **2018**, *24*, 3305-3313.

[17] a) Y. D. Liu and S. Kumar, *Polym. Rev.* **2012**, *52*, 234–258; b) X. S. Huang, *Materials* **2009**, *2*, 2369-2403.

[18] D. M. Morgan, *Surf. Interface Anal.* **2015**, *47*, 1072-1079.

[19] Commercial carbon fiber, http://www.clipcarbono.com/es/home/266-tejido-de-fibra-de-carbono-sarga-2×2-3k-peso-200gr-m2-ancho-1200-mm.html.

WILEY-VCH

Entry for the Table of Contents

FULL PAPER

Four heterogeneous hybrid cathodes for the catalytic hydrogen evolution reaction (HER) have been prepared combining two types of carbon fibers and two different synthetic methodologies to decorate their surfaces with Ru nanoparticles. The activity and stability of all the hybrid systems has been evaluated.

Artificial Photosynthesis

Jordi Creus, Laura Mallón, Nuria Romero, Roger Bofill, Alicia Moya, Jose L. G. Fierro, Rubén Mas-Ballesté*, Xavier Sala, Karine Philippot*, Jordi García-Antón*

Page No. – Page No.

Ruthenium Nanoparticles Supported onto Carbon Microfibers for Hydrogen Evolution Electrocatalysis

[1] *BP Energy Outlook* **2018**, BP Global.

[2] V. Scott, R. S. Haszeldine, S. F. B. Tett, A. Oschlies, *Nat. Clim. Change* **2015**, *5*, 419-423.

[3] N. S. Lewis, *Nature* **2001**, *414*, 589-590.

[4] S. Berardi, S. Drouet, L. Francàs, C. Gimbert-Suriñach, M. Guttentag, C. Richmond, T. Stoll, A. Llobet, *Chem. Soc. Rev.* **2014**, *43*, 7501-7519.

[5] a) S. Trasatti, *J. Electroanal. Chem.* **1972**, *39*, 163-184; b) C. C. L. McCrory, S. Jung, I. M. Ferrer, S. M. Chatman, J. C. Peters, T. F. Jaramillo, *J. Am. Chem. Soc.* **2015**, *137*, 4347-4357; c) J. K. Norskov, T. Bligaard, A. Logadottir, J. R. Kitchin, J. G. Chen, S. Pandelov, U. Stimming, *J. Electrochem. Soc.* **2005**, *152*, J23-J26.

[6] a) N. Coutard, N. Kaeffer, V. Artero, *Chem. Commun.* **2016**, *52*, 13728-13748; b) A. Eftekhari, *Int. J. Hydrogen Energy* **2017**, *42*, 11053-11077.

[7] a) Y. G. Li, H. L. Wang, L. M. Xie, Y. Y. Liang, G. S. Hong, H. J. Dai, *Am. Chem. Soc.* **2011**, *133*, 7296-7299; b) E. J. Popczun, J. R. McKone, C.G. Read, A. J. Biacchi, A. M. Wiltrout, N. S. Lewis, R. E. Schaak, *J. Am. Chem. Soc.* **2013**, *135*, 9267-9270; c) T. F. Jaramillo, K. P. Jorgensen, J. Bonde, J. H. Nielsen, S. Horch, I. Chorkendorff, *Science* **2007**, *317*, 100–102; d) J. R. McKone, B. F. Sadtler, C. A. Werlang, N. S. Lewis, H. B. Gray, *ACS Catal.* **2013**, *3*, 166-169; e) L. Liao, S. N. Wang, J. J. Xiao, X. J. Bian, Y. H. Zhang, M. D. Scanlon, X. L. Hu, Y. Tang, B. H. Liu, H. H. Girault, *Energy Environ. Sci.* **2014**, *7*, 387-392.

[8] M. Zheng, Y. Li, *J. Mater. Chem.* A **2015**, *3*, 14942-14962.

[9] a) J. Mahmood, F. Li, S. Jung, M. S. Okyay, I. Ahmad, S. Kim, N. Park, H. Y. Jeong, J. Baek, *Nature Nanotech.* **2017**, *12*, 441-446; b) T. Bhowmik, M. K. Kundu, S. Barman, *ACS Appl. Mater. Interfaces* **2016**, *8*, 28678-28688; c) J. Cheng, H. Zhang, H. Ma, H. Zhong, Y. Zou, *Electrchim. Acta* **2010**, *55,* 1855-1861; d) X. Kong, K. Xu, C. Zhang, J. Dai, S. N. Oliaee, L. Li, X. Zeng, C. Wu, Z. Peng, *ACS Catal.* **2016**, *6*, 1487-1492; e) Y. Zheng, Y. Jiao, Y. Zhu, L. H. Li, Y. Han, Y. Chen, M. Jaroniec, S. Qiao, *J. Am. Chem. Soc.* **2016**, *138*, 16174-16181; f) Z. Chen, J. Lu, Y. Ai, Y. Ji, T. Adschiri, L. Wan *ACS Appl. Mater. Interfaces* **2016**, *8*, 35132-35137.

[10] a) Y. Zhang, T. Ren, *Chem. Commun.* **2012**, *48*, 11005-11007; b) N. C. King, C. Dickinson, W. Zhou, D. W. Bruce, *Dalton Trans.* **2005**, *6*, 1027-1032; c) K. P. J. Gustafson, A. Shatskiy, O. Verho, M. D. Kärkäs, B. Schluschass, C. Tai, B. Åkermark, J. Bäckvall, E. V. Johnston, *Catal. Sci. Technol.* **2017**, *7*, 293-299.

[11] a) J. Liu, Y. Zheng, D. Zhu, A. Vasileff, T. Ling, S. Z. Qiao, *Nanoscale* **2017**, *9*, 16616-16621; b) P. Jiang, Y. Yang, R. Shi, G. Xia, J. Chen, J. Su, Q. Chen, *J. Mater. Chem. A* **2017**, *5*, 5475-5485; c) U. Joshi, S. Malkhandi, Y. Ren, T. L. Tan, S. Y. Chiam, B. S. Yeo, *ACS Appl. Mater. Interfaces* **2018**, *10*, 6354-6360; d) L. Zhu, Q. Cai, F. Liao, M. Sheng, B. Wu, M. Shao, *Electrochem. Commun.* **2015**, *52*, 29-33; e) E. Demir, S. Akbayrak, A. M. Önal, S. Özkar, *ACS Appl. Mater. Interfaces* **2018**, *10*, 6299-6308.

[12] a) K. Magdić, K. Kvastek, V. Horvat-Radošević, *Electrochim. Acta* **2015**, *167*, 455-469; b) R. K. Shervedani, A. Amini, *Carbon* **2015**, *93*, 762-773.

[13] S. Drouet, J. Creus, V. Collière, C. Amiens, J. García-Antón, X. Sala, K. Philippot, *Chem. Commun.* **2017**, *53*, 11713-11716.

[14] J. Creus, S. Drouet, S. Suriñach, P. Lecante, V. Colliere, R. Poteau, K. Philippot, J. García-Antón, X. Sala, *ACS Catal.* **2018**, *8*, 11094-11102.

[15] C. Amiens, B. Chaudret, D. Ciuculescu-Pradines, V. Collière, K. Fajerwerg, P. Fau, M. Kahn, A. Maisonnat, K. Soulantica, K. Philippot, *New J. Chem.* **2013**, *37*, 3374-3401.

[16] O. González-del Moral, A. Call, F. Franco, A. Moya, J. A. Nieto-Rodríguez, M. Frías, J. L. G. Fierro, M. Costas, J. Lloret-Fillol, J. Alemán, R. Mas-Ballesté, *Chem. Eur. J.* **2018**, *24*, 3305-3313.

[17] a) Y. D. Liu and S. Kumar, *Polym. Rev.* **2012**, *52*, 234–258; b) X. S. Huang, *Materials* **2009**, *2*, 2369-2403.

[18] D. M. Morgan, *Surf. Interface Anal.* **2015**, *47*, 1072-1079.

[19] Commercial carbon fiber, http://www.clipcarbono.com/es/home/266-tejido-de-fibra-de-carbono-sarga-2×2-3k-peso-200gr-m2-ancho-1200-mm.html.